Light-induced degradation and metastable-state recovery with reaction kinetics modeling in boron-doped Czochralski silicon solar cells

Soo Min Kim,[1] Seungju Chun,[1] Suhyun Bae,[1] Seungeun Park,[1] Min Gu Kang,[2] Hee-eun Song,[2] Yoonmook Kang,[3,a)] Hae-seok Lee,[1,b)] and Donghwan Kim[1,c)]
[1]*Department of Materials Science and Engineering, Korea University, Anam-dong, Seongbuk-gu, Seoul 136-701, South Korea*
[2]*Korea Institute of Energy Research, 152 Gajeong-ro, Yuseong-gu, Daejeon 305-343, South Korea*
[3]*KU-KIST Green School, Graduate School of Energy and Environment, Korea University, Anam-dong, Seongbuk-gu, Seoul 136-701, South Korea*

(Received 16 June 2014; accepted 19 August 2014; published online 28 August 2014)

Solar cells fabricated from boron-doped p-type Czochralski silicon suffer from light-induced degradation that can lower the conversion efficiency by up to 10% relative. When solar cells are exposed to temperatures between 100 °C and 200 °C under illumination, regeneration, in which the minority carrier lifetime is gradually recovered, occurs after the initial light-induced degradation. We studied the light-induced degradation and regeneration process using carrier injection within a design chamber and observed open-circuit voltage trends at various sample temperatures. We proposed a cyclic reaction kinetics model to more precisely analyze the degradation and recovery phenomenon. Our model incorporated the reaction paths that were not counted in the original model between the three states (annealed, degradation, and regeneration). We calculated a rate constant for each reaction path based on the proposed model, extracted an activation energy for each reaction using these rate constants at various temperatures, and calculated activation energies of redegradation and the stabilization reaction. © *2014 AIP Publishing LLC*.
[http://dx.doi.org/10.1063/1.4894289]

The conversion efficiency of solar cells fabricated of boron-doped Czochralski (Cz) silicon substrate is degraded when the cells are exposed to sunlight or carriers are injected in the dark condition, and recently considerable research has been focused on this light-induced degradation (LID) problem.[1,2] In 1974, Fischer and Pschunder reported LID for the first time and showed that recovery back to the annealed state from a fully degraded solar cell took 10 min of annealing at 200 °C in the dark condition.[3] Nowadays, conventional crystalline silicon solar cells based on boron-doped Cz-Si wafers reach an ultra-high conversion efficiency range (20%–21%), so LID effects can no longer be ignored. Ultra-high-efficiency solar cells such as the passivated emitter rear locally diffused (PERL) solar cells of the university of new south wales (UNSW) suffered performance degradation of about 10% on the laboratory scale.[4–6] A main cause of LID is known to result from a boron oxide complex (B_sO_{2i}), comprising a substitutional boron (B_s) and an interstitial oxygen dimer (O_{2i}), which degrades the minority carrier lifetime by self-trapping-enhanced carrier recombination mechanism.[2,7,8]

Recently, Herguth *et al.* reported a kind of permanent recovery phenomenon.[9,10] When a solar cell is continuously exposed to sunlight at >90 °C, initially, the minority carrier lifetime of the solar cell was reduced by LID effects; however, as time passes, a slow recovery (regeneration) occurs. This regeneration state exhibits about an 80% recovery of the minority carrier lifetime of the annealed-state condition; a slight decrease in lifetime occurs initially under illumination at room temperature but no more additional degradation occurs.[11] However, when a solar cell under the regeneration state is annealed at >100 °C in a dark or light environment, the regeneration state gradually transitions to a LID state, indicating that the regeneration reaction condition is not maintained permanently.[10] Studies of the causative agent for the regeneration state are in progress to analyze the detailed recombination mechanism, but the agent has not been accurately identified until now. Moreover, it has been reported that LID and the regeneration state occur when a reverse bias or light bias state is applied to a solar cell under the dark condition.[10]

These reports indicate that carrier injection rather than the light itself is known to play an important role. To explain the kinetic properties of LID and regeneration as functions of time, Herguth *et al.* have constructed the consecutive reversible reaction models to define the portion of each state (e.g., annealed (state A), degradation (state B), and regeneration (state C)) by making a few assumptions. First, the reaction rate constant for the destabilization process, which is the state change from regeneration to annealed, is assumed to be zero because this reaction path has not been observed. For the same reason, the reaction rate constant of stabilization (A → C), which is the reverse reaction of destabilization (C → A) and redegradation (C → B), the latter of which returns to the LID state, is also assumed to have zero value.[12–14] As a result of these assumptions, the final state of the minority carrier lifetime for the solar cell reaches the 100% regeneration state after a relatively long time, exhibiting little difference between calculation and experimental results in a total reaction kinetics plot.

a)ddang@korea.ac.kr
b)lhseok@korea.ac.kr
c)donghwan@korea.ac.kr

In this study, we assumed that redegradation, destabilization, and stabilization can occur in continuous experimental reactions at high temperature and under a reverse bias condition to reflect previous experimental results that show recovery of minority carrier lifetime of about 80% as compared with the annealed state obtained from calculations of a reaction kinetics model for a saturated regeneration state. Therefore, we proposed to incorporate in the calculation all the six reaction paths between the three states to better analyze the series of reactions after the sunlight irradiation. We call this the cyclic kinetics reaction model.

We performed experimental regeneration in which we adjusted the reverse bias intensity and specimen temperature without a light source to remove noise from the signal owing to instability of the light intensity when the light source continuously irradiated the solar cell. We extracted the activation energies of redegradation, stabilization, and destabilization processes using the proposed reaction kinetics model.

We used 156 mm × 156 mm pseudo-square boron-doped p-type Cz-si wafers with (100) orientation (200 μm in thickness, with resistivity of 1.0 ~ 2.0 Ω-cm) to fabricate our solar cell. The interstitial oxygen concentrations (O_i) and substitutional carbon concentration (C_s) were measured by Fourier transform infrared spectroscopy and were 8.05×10^{17} and $2.48 \times 10^{16}\,cm^{-3}$, respectively, in the wafer. We observed the reaction rates as a function of carrier injection density and temperature of the specimen by fixing the average concentration range of oxygen and carbon impurities. The solar cell was fabricated by using a conventional screen printing process; a silicon nitride (SiN_x) layer was deposited by plasma enhanced chemical vapor deposition as an antireflection coating on the front side. We used a belt furnace system for the electrode firing process; the front silver grid and rear aluminum full electrode patterns were printed by an autoalignment screen printer.

We designed an enclosed chamber to minimize the influence of outside light or external temperature. The chamber consisted of a thermal source to control specimen temperature, a device to monitor the sample surface temperature, and a device to measure electrical properties such as current and voltage. We installed a ceramic heating coil under the sample plate to adjust the temperature of the specimen; the sample temperature could be controlled between 380 ± 0.1 °C and −10 ± 0.1 °C with an inner circulation coolant system. We used an infrared temperature monitor system to limit the response time to <0.1 s because even a minimal change of sample temperature can affect the open-circuit voltage in a proportional–integral–derivative–controlled (PID) environment. We fabricated a vacuum hole inside of the sample plate to improve contact and maintain a uniform temperature gradient throughout the total sample area. Furthermore, we designed a 30-point contact probe station to advance the front electrode contact. A SMU (Keithley 238) was used to control the injection current or voltage and to observe the electrical properties in the solar cell. The measurement interval for electrical properties was maintained at 0.005 s, and the bias ranges adopted were 1.0 nA–1.0 A (current) and 1.0 μV to 10.0 V (voltage).

The sample was annealed at 200 °C for 15 min in the dark state to remove boron oxide complex (B_sO_{2i}) before the experiment. The solar cell temperature was then dropped to regeneration conditions such as at annealing temperatures of 100, 120, 130, and 150 °C and maintained for 10 min to prevent thermal instability for recombination. A reverse current bias (0.9 A) was applied to the solar cell under a target temperature (±0.1 °C), and voltage values were recorded at time intervals of 0.2 s for 100 s of experimental time and then at intervals of 1 ~ 10 s afterward. When the monitored *in situ* voltage change remained <10 μV for a few hours, we stopped the experiment.

In this study, we assumed that the annealed, degradation, and regeneration states were defined by formation and dissociation of some chemical complex. In Fig. 1, the LID complex density is calculated through the normalized defect concentration (NDC): $N_t^*(t) = 1/V(t) - 1/V(0)$, where $V(t)$ and $V(0)$ are the voltage values at t and t = 0, respectively. When a reverse current of 0.9 A was applied to the solar cell at 100 °C, regeneration increased with increasing NDC in the short-term, but a decreasing trend is evident after a certain period of time. A schematic diagram of the overall reaction process is shown in Fig. 1, with annealed, degradation, and regeneration states defined as states A, B, and C, respectively.

The forward direction of the reaction path is denoted as k_i ($i = 1, 2, 3$), and the inverse reaction path is defined as k_{ij} ($j = 1, 2, 3$). In the annealed state, we assumed that there were no boron atoms in substitutional sites connected with any oxygen dimers because of the initial annealing treatment. We assumed that the B_sO_{2i} complex arises as a result of the LID process and then migrates to a third state, such as another phase of the complex or atomic arrangement, during the regeneration process. Therefore, the activation energy of each reaction step can be extracted by using the proposed model because a portion of each state changes with time. The governing equations of the cyclic reaction kinetics model are defined by

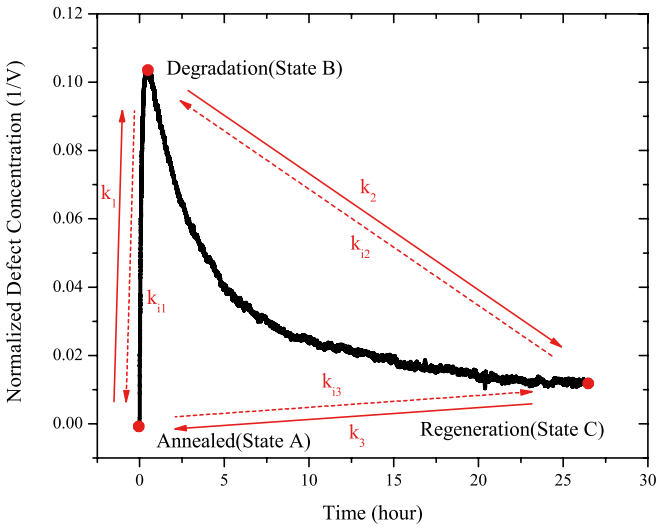

FIG. 1. Normalized defect concentration (N^*) for the degradation and regeneration process with open-circuit voltage and a schematic diagram for the cyclic reaction kinetics model. k_i ($i = 1, 2$, and 3) denote degradation, regeneration, and destabilization and k_{ij} ($j = 1, 2$, and 3) denote recovery, redegradation, and stabilization.

$$\frac{\partial C_a}{\partial t} = k_3 C_c - k_{i3} C_a - k_1 C_a + k_{i1} C_b, \quad (1a)$$

$$\frac{\partial C_b}{\partial t} = k_1 C_a - k_{i1} C_b - k_2 C_b + k_{i2} C_c, \quad (1b)$$

$$\frac{\partial C_c}{\partial t} = k_2 C_b - k_{i2} C_c - k_3 C_c + k_{i3} C_a, \quad (1c)$$

where C_i $(i = a, b, c)$ are the densities of each state for states A, B, and C, and reaction constants are represented by k_i $(i = 1, 2, 3)$ and k_{ij} $(j = 1, 2, 3)$. We used an eigenvalue method to solve these governing equations, defining the following equations:[15]

$$C_a = J_a e^{-\lambda t}, \quad (2a)$$

$$C_a' = -\lambda J_a e^{-\lambda t}. \quad (2b)$$

Eq. (2) can be used to redefine Eq. (1) as follows:

$$\lambda J_a - k_{i3} J_a - k_1 J_a + k_{i1} J_b + k_3 J_c = 0, \quad (3a)$$

$$k_1 J_a + \lambda J_b - k_{i1} J_b - k_2 J_b + k_{i2} J_c = 0, \quad (3b)$$

$$k_{i3} J_a + k_2 J_b + \lambda J_c - k_{i2} J_c - k_3 J_c = 0, \quad (3c)$$

which can be expressed as the following matrix formula to solve the eigenvalue problem:

$$\begin{pmatrix} \lambda - k_{i3} - k_1 & k_{i1} & k_3 \\ k_1 & \lambda - k_{i1} - k_2 & k_{i2} \\ k_{i3} & k_2 & \lambda - k_{i2} - k_3 \end{pmatrix} \begin{pmatrix} J_a \\ J_b \\ J_c \end{pmatrix} = 0. \quad (4)$$

Taking the determinant of the first part of the left side in Eq. (4), we can identify three λ values. We can calculate J_j $(j = a, b, c)$ values and substitute the calculated λ values into Eq. (3). The general solution can be extracted through the calculated λ_i $(i = 1, 2, 3)$ and $J_{j,i}$ $(i = 1, 2, 3, j = a, b, c)$ values. The fully expanded formula using general solution shows the concentration of each state as a function of time

$$C_i = J_{i,1} e^{-\lambda_1 t} + J_{i,2} e^{-\lambda_2 t} + J_{i,3} e^{-\lambda_3 t} \ (i = a, b, c). \quad (5)$$

We assumed a recovery process in which perfect dissociation of recombination occur in the experiment in this study, so the concentration of state A is defined as 100% at t = 0 and those at states B and C are 0% ($C_{a,0} = 100$, $C_{b,0} = 0$, and $C_{c,0} = 0$). We can then calculate the open-circuit voltage trends during the experiment by inputting the rate constants k_i $(i = 1, 2, 3)$ and k_{ij} $(j = 1, 2, 3)$, which induce degradation and regeneration as time passes.

Fig. 2 shows the open-circuit voltage trend at various temperatures under the condition of 0.9 A of reverse current bias. Because it is hard to directly compare solar cells at different temperatures because the energy band gap of silicon affects thermal energy, we calculate the normalized open-circuit voltage (NVOC), $V^* = V(t)/V(0) \times 100(\%)$, where $V(t)$ and $V(0)$ are the voltage values at t and t = 0, respectively. In Fig. 2, the normalized open-circuit voltage of state B, which is the lowest position of the open-circuit voltage, is 95% ($\Delta V = 18.6$ mV) at 373 K and 99% ($\Delta V = 3.8$ mV) at 423 K. The reason for the increasing state B position is that the LID rate of the solar cell increases rapidly with increasing

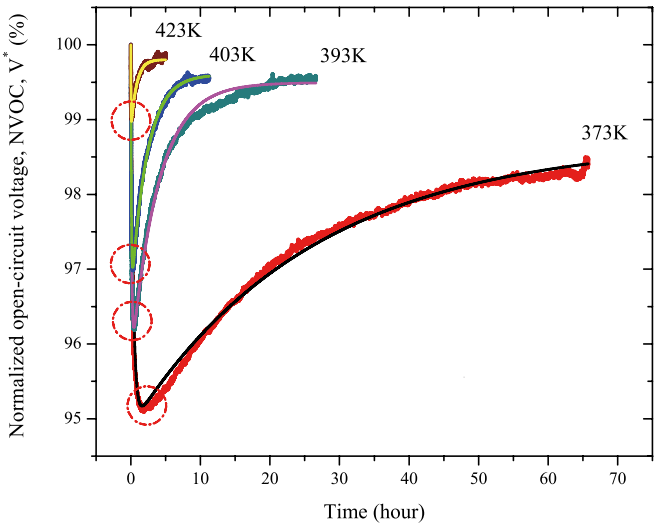

FIG. 2. Experimentally observed NVOC (V^*) with multiple samples and cyclic reaction kinetics calculation at various temperatures. The thin smooth solid lines are the calculated results from cyclic reaction kinetics modeling.

temperature, but recovery (dissociation and regeneration) processes are much faster than degradation. The arrival time of the regeneration state increases by a factor of: 13 from 5 h at 423 K to 65 h at 373 K. Moreover, although the regeneration rate is much faster as sample temperature increases, when the solar cell reached 423 K, state C shows an unstable saturation value like a broad-amplitude sine wave. At high temperature, we suspect that it is hard to maintain a saturated compensation rate composed of regeneration and stabilization processes and redegradation and destabilization processes for state C.

In Fig. 2, we compared our experimental data and calculation results using the cyclic reaction kinetics model defined by Eq. (5). Our calculated results agree well with experimental data and are highly precise at 373 K, exhibiting good reliability for open-circuit voltage trends with increasing temperature. According to Eq. (5), six reaction rate constants corresponding to transfer rates between each state could be extracted by matching experimental data and calculated results with various temperatures. The activation energy of each reaction path could be calculated from the reaction constants by using the Arrhenius equation: $\mathrm{Log}(k) = \mathrm{Log}(A) - E_a/(2.30259 \times k_b \times T)$, where k is the reaction rate constant, A is a frequency factor that has the same units as the rate constant, the activation energy is E_a, and k_b is the Boltzmann constant. In Fig. 3, we calculated the activation energy of LID with temperature-dependence rate constants k_1. Plotting those reaction rates against inverse temperature allows us to extract an activation energy of 0.38 ± 0.03 eV, which agrees well with results from other groups.[8,16] Table I shows the activation energy of each reaction step with the extracted reaction rate constants found using the same calculation method compared to values from existing reports.

In our results, the activation energy of the regeneration process is 0.90 ± 0.07 eV, which is different from that of other groups, but for the destabilization process, our results (1.09 ± 0.10 eV) agree well.[9,10,12,17] The degradation and destabilization processes (k_i $(i = 1, 3)$) present similar results compared with existing reports. However, a huge difference

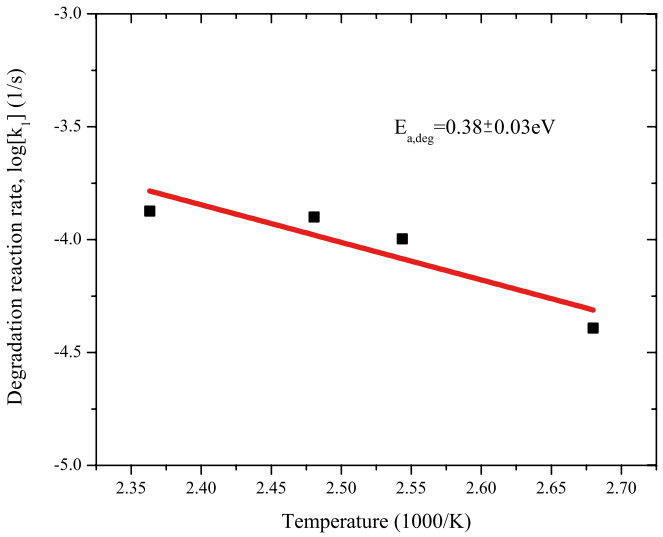

FIG. 3. Arrhenius plot of the defect degradation rate (k_{i1}). The activation energy of the degradation process is $E_{a,deg} = 0.38 \pm 0.03$ eV.

is evident in the recovery process (k_{i1}) between our results and those of others. The reasons for these differences in the activation energy are believed to be due to the different assumptions in the kinetics model.[18] We thought that the differences in recovery processes from those of other groups are due to the reaction kinetics model of *state A* $\rightleftarrows$ *state B* $\rightleftarrows$ *state C* $\rightleftarrows$ *state A* by supposing state C in this study.

Furthermore, we were able to calculate the unknown activation energies of reaction steps such as redegradation (k_{i2}) and stabilization (k_{i3}) in previous research. From those results, we suggested that there is a direct transformation path between state A and state C. After reaching the saturation point, it can be explained little concentration of state A through destabilization process within state C that some LID occurred in a short time when the solar cell was exposed to sunlight at room temperature. Destabilization, however, which means a transfer from regeneration to annealed states, is difficult under light bias and high temperature because the activation energy required for the destabilization reaction is: 1.0 eV greater than that for the regeneration process. Therefore, the internal defects of the solar cell under light bias and high temperature consist mostly of the regeneration state, with the cyclic reaction kinetics model entering into a steady state after much time.

In this study, we observed open-circuit voltage trends through a real-time monitoring method when a solar cell was exposed to high-temperature conditions under a minority carrier injection state. We traced the open-circuit voltage trends and analyzed the regeneration process using a cyclic reaction kinetics model for six reaction paths. The required reaction rate constant was calculated by using the proposed model at various sample temperatures. We calculated the activation energy of each reaction path using rate constants as a function of temperature. We tried to explain the light-induced degradation process and regeneration phenomenon, and calculated the activation energies of redegradation and stabilization.

TABLE I. Extracted activation energies of reaction paths from the cyclic reaction kinetics model.

	E_a (eV)	Reference values (eV)
Degradation (k_1)	0.38 ± 0.03	0.3 (Ref. 8) 0.37 (Ref. 16) 0.39 ± 0.05 (Ref. 19) 0.4 (Ref. 20) 0.44 ± 0.07 (Ref. 9) 0.45 (Refs. 9, 21, and 22) 0.47 (Ref. 23) 0.475 ± 0.035 (Ref. 24)
Regeneration (k_2)	0.90 ± 0.07	0.62 ± 0.02 (Ref. 9) 0.64 ± 0.04 (Ref. 10)[a] 0.61 ± 0.01 (Ref. 10)[b] 0.69 ± 0.06 (Ref. 17)[c] 0.7 (Ref. 12) 0.72 ± 0.007 (Ref. 17)[d]
Destabilization (k_3)	1.09 ± 0.10	1.00 ± 0.03 (Refs. 9 and 10)[e] 0.98 ± 0.01 (Refs. 9 and 10)[f]
Recovery (k_{i1})	0.78 ± 0.06	1.24 (Ref. 25) 1.3 (Refs. 18 and 22) 1.32 (Ref. 26) 1.36 ± 0.08 (Ref. 24) 1.32 ± 0.05 (Ref. 24)
Redegradation (k_{i2})	0.51 ± 0.01	None
Stabilization (k_{i3})	1.07 ± 0.14	None

[a]Minority carrier lifetime measure.
[b]Quasi-neutral region saturation current density(J_{01}) measure.
[c]Bare wafer measure.
[d]Phosphorus diffusion wafer measure.
[e]Short-circuit current density (J_{sc}) measure.
[f]Open-circuit voltage (V_{oc}) measure.

This work was supported by the New & Renewable Energy Core Technology Program of the Korea Institute of Energy Technology Evaluation and Planning (KETEP) granted financial from the Ministry of Trade, Industry & Energy, Republic of Korea (No. 20133010011760).

[1]S. W. Glunz, S. Rein, J. Y. Lee, and W. Warta, "Minority carrier lifetime degradation in boron-doped Czochralski silicon," J. Appl. Phys. **90**(5), 2397–2404 (2001).
[2]V. G. Weizer, H. W. Brandhorst, J. D. Broder, R. E. Hart, and J. H. Lamneck, "Photon-degradation effects in terrestrial silicon solar cells," J. Appl. Phys. **50**(6), 4443–4449 (1979).
[3]H. Fischer and W. Pschunder, "Investigation of photon and thermal induced changes in silicon solar cells," in *Proceedings of 10th IEEE Photovoltaic Specialists Conference* (1974), p. 404.
[4]J. H. Zhao, A. H. Wang, M. A. Green, and F. Ferrazza, "19.8% efficient "honeycomb" textured multicrystalline and 24.4% monocrystalline silicon solar cells," Appl. Phys. Lett. **73**(14), 1991–1993 (1998).
[5]J. Knobloch, S. Glunz, V. Henninger, W. Warta, W. Wettling, F. Schomann, W. Schmidt, A. Endros, and K. A. Müzer, "21% efficient solar cells processed from Czochralski grown silicon," in *Proceedings of 13th European PVSEC* (1995), pp. 9–12.
[6]S. Sterk, K. Müzer, and S. Glunz, "Investigation of the degradation of crystalline silicon solar cells," in *Proceedings of 14th European PVSEC* (1997), pp. 85–87.
[7]X. Chen, X. Yu, X. Zhu, P. Chen, and D. Yang, "First-principles study of interstitial boron and oxygen dimer complex in silicon," Appl. Phys. Express **6**(4), 041301 (2013).
[8]M.-H. Du, H. M. Branz, R. S. Crandall, and S. B. Zhang, "A new mechanism for non-radiative recombination at light-induced boron-oxygen

complexes in silicon," paper presented at the 2005 DOE Solar Energy Technologies Program Review Meeting, November 2005.
[9]A. Herguth, G. Schubert, M. Kaes, and G. Hahn, "A new approach to prevent the negative impact of the metastable defect in boron doped cz silicon solar cells," in *Proceedings of IEEE 4th World Conference Photovoltaic Energy Conversion* (2006), Vol. 1, pp. 940–943.
[10]A. Herguth, G. Schubert, M. Kaes, and G. Hahn, "Avoiding boron-oxygen related degradation in highly boron doped Cz silicon," in Proceedings of 21st European PVSEC (2006).
[11]B. Lim, S. Hermann, K. Bothe, and J. Schmidt, "Permanent deactivation of the boron-oxygen recombination center in silicon solar cells," in Proceedings of 23rd European PVSEC (2008).
[12]A. Herguth, G. Schubert, M. Kaes, and G. Hahn, "Investigations on the long time behavior of the metastable boron-oxygen complex in crystalline silicon," Prog. Photovoltaics **16**(2), 135–140 (2008).
[13]A. Herguth and G. Hahn, "Boron-oxygen related defects in Cz-silicon solar cells degradation, regeneration and beyond," in *Proceedings of 24th European PVSEC* (2009), pp. 974–976.
[14]A. Herguth and G. Hahn, "Kinetics of the boron-oxygen related defect in theory and experiment," J. Appl. Phys. **108**(11), 114509 (2010).
[15]K. A. Connors, *Chemical Kinetics. The Study of Reaction Rates in Solution* (VCH Publishers, Inc., 2014).
[16]K. Bothe, R. Hezel, and J. Schmidt, "Understanding and reducing the boron-oxygen-related performance degradation in Czochralski silicon solar cells," Solid State Phenom. **95–96**, 223–228 (2004).
[17]B. Lim, K. Bothe, and J. Schmidt, "Deactivation of the boron-oxygen recombination center in silicon by illumination at elevated temperature," Phys. Status Solidi RRL **2**(3), 93–95 (2008).
[18]J. Schmidt and K. Bothe, "Structure and transformation of the metastable boron- and oxygen-related defect center in crystalline silicon," Phys. Rev. B **69**(2), 024107 (2004).
[19]S. Dubois, N. Enjalbert, and J. P. Garandet, "Slow down of the light-induced-degradation in compensated solar-grade multicrystalline silicon," Appl. Phys. Lett. **93**(10), 103510 (2008).
[20]J. Schmidt, K. Bothe, and R. Hezel, "Formation and annihilation of the metastable defect in boron-doped Czochralski silicon," in *Proceedings of 29th IEEE Photovoltaic Specialists Conference* (2002), pp. 178–181.
[21]S. W. Glunz, E. Schaeffer, S. Rein, K. Bothe, and J. Schmidt, "Analysis of the defect activation in Cz-silicon by temperature-dependent bias-induced degradation of solar cells," in *Proceedings of the 3rd World Conference on Photovoltaic Energy Conversion* (2003), p. 919.
[22]J. Schmidt, A. G. Abele, and R. Hezel, "Formation and annihilation of the metastable defect in boron doped Czochralski silicon," in *Proceedings of the 29th IEEE Photovoltaic Specialists Conference* (2002), p. 178.
[23]D. W. Palmer, K. Bothe, and J. Schmidt, "Kinetics of the electronically stimulated formation of a boron-oxygen complex in crystalline silicon," Phys. Rev. B **76**(3), 035210 (2007).
[24]K. Bothe and J. Schmidt, "Electronically activated boron-oxygen-related recombination centers in crystalline silicon," J. Appl. Phys. **99**(1), 013701 (2006).
[25]J. Adey, R. Jones, D. W. Palmer, P. R. Briddon, and S. Oberg, "Degradation of boron-doped Czochralski-grown silicon solar cells," Phys. Rev. Lett. **93**(5), 055504 (2004).
[26]S. Rein, T. Rehrl, W. Warta, S. W. Glunz, and G. Willeke, "Electrical and thermal properties of the metastable defect in boron-doped Czochralski silicon (Cz-Si)," in *Proceedings of the 17th European Photovoltaic Solar Energy Conference* (2001), p. 1555.